Solid Freeform Fabrication 2024: Proceedings of the 35th Annual International
Solid Freeform Fabrication Symposium – An Additive Manufacturing Conference

PHOTOCURABLE SLA RESIN FORMULATION FOR REDUCED COEFFICIENT OF THERMAL EXPANSION

Muhammad A. Sufian[1], Rahul R. Sheley[1,2], and Jitendra Tate*,[1,2]

Texas State University
601 University Drive, San Marcos, TX,78666
[1] Ingram School of Engineering
[2] Materials Science Engineering and Commercialization Program,
Email: JT31@txstate.edu

ABSTRACT

Despite its commendable resolution capabilities, Stereolithography 3D Printing (SLA) often falls short in achieving desired material properties compared to alternative additive manufacturing techniques. To address this limitation, one strategy involves nickel electroplating of printed parts, thereby enhancing mechanical strength, heat resistance, and chemical durability. However, this approach introduces a discrepancy in the coefficient of thermal expansion (CTE) between the resin and the nickel coating, leading to internal stresses and potential part failure when subjected to high-temperature fluctuations. In this work, we reported the successful development of a noble SLA resin using pre-dispersed amorphous silicon dioxide in cycloaliphatic epoxy resin that offers high modulus, high strength, low density, and low Coefficient of Thermal Expansion (CTE). Tensile analysis revealed that silica incorporation improves stiffness by 74% while reducing tensile strength by around 13%. Flexural tests showed enhanced bending resistance, particularly at 5 wt% silica loading. Thermal analysis confirmed a 25% reduction in CTE with silica addition, making the 5 wt% SiO_2 resin an optimal choice for applications requiring mechanical durability and thermal stability.

Keywords: nanocomposites; stereolithography 3D printing; silica nanoparticles; coefficient of thermal expansion; mechanical properties;

1. INTRODUCTION

Stereolithography (SLA) is a well-established additive manufacturing technique that allows for the fabrication of highly detailed and complex 3D structures with exceptional precision [1-3]. The process begins with the application of a thin layer of a photocurable resin onto a platform. A focused UV laser, guided by computer-generated models, selectively cures specific regions of the resin, forming a solid layer corresponding to the desired cross-sectional geometry [4,5]. Once the layer is cured, the platform descends to allow the deposition of a new layer of resin, and the process is repeated until the entire object is fabricated. This layer-by-layer construction provides remarkable design flexibility and is widely used in industries where accuracy and intricate detailing are critical.

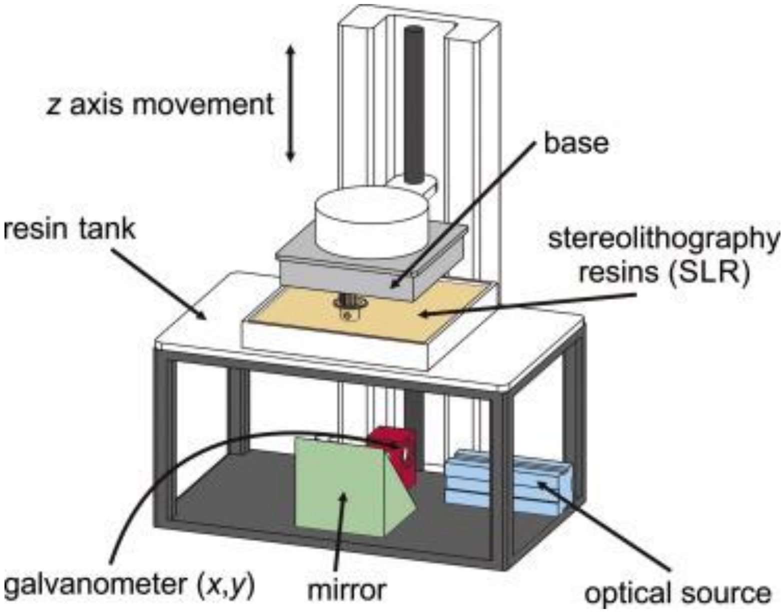

Figure 1: SLA printing process [6]

While stereolithography (SLA) has emerged as a powerful tool for fabricating complex and highly detailed components, parts manufactured using SLA resin often exhibit inferior mechanical properties compared to traditional manufacturing methods. Specifically, SLA parts tend to have lower strength, reduced thermal stability, and increased brittleness due to the inherent characteristics of photocurable resins. Polymers also generally exhibit lower strength and elastic modulus than metals, limiting their use for critical structural applications. Surface treatments such as nickel coating have been employed to address these limitations and enhance the durability of SLA-fabricated components. Nickel plating not only improves the mechanical strength and wear resistance of the parts but also provides a protective barrier against environmental factors such as corrosion and high-temperature fluctuations. This surface modification technique is critical for applications requiring higher performance and long-term reliability in challenging environments.

A significant issue arises when there is a mismatch between the coefficient of thermal expansion (CTE) of nickel coatings and the commercially available stereolithography (SLA) resins. Typical SLA resins have a CTE ranging from 80 to 100 × 10^{-6} µm/°C, while nickel exhibits a much lower CTE of approximately 13 × 10^{-6} µm /°C. This disparity in thermal expansion rates leads to considerable internal stresses within the printed parts, particularly when exposed to high-temperature gradients. As the temperature fluctuates, the resin and nickel coating expand or contract at different rates, causing potential warping, delamination, or even cracking of the part. These thermal stresses can compromise the structural integrity and dimensional accuracy of the printed components, especially in applications where consistent thermal performance is critical. Therefore, addressing this CTE mismatch is essential for enhancing the reliability of SLA-fabricated parts coated with nickel.

The use of nano-fillers to achieve enhanced material properties, including the reduction of the coefficient of thermal expansion (CTE), has garnered significant interest among researchers in recent years. Incorporating fillers into polymer matrices is a widely adopted strategy for tailoring thermal and mechanical properties. For instance, epoxy molding compounds typically contain over 60 wt% silica fillers to reduce CTE [7]. Among these, nano-fillers with a high aspect ratio are particularly effective in reducing CTE along the longitudinal axis due to their elongated structure, which restricts thermal expansion [8, 9]. Commonly used fillers to lower the CTE of polymers include silica compounds [10], titanium oxide [11], aluminum compounds [12], and Zirconium Tungstate (ZrW_2O_8) [13]. Despite the extensive use of silica in traditional composites, the effect of pre-dispersed colloidal nano-silica on the CTE of epoxy-based stereolithography resins (SLR) has not been thoroughly investigated. Nano-silica is especially promising due to its high surface area and excellent dispersion capability, which enhances interaction with the resin matrix and contributes to better thermal stability. This study explores the potential of nano-silica in reducing the CTE of SLA resins, offering a novel approach to overcoming the challenges associated with thermal expansion in SLA 3D-printed parts.

2. MATERIALS AND METHODS

2.1 Materials

In the experiments, the resin formulations primarily consisted of three components: an oligomer, a monomer, and two photo-initiators. The oligomer used was a commercially available epoxy-based resin, known for its superior mechanical properties, high accuracy, and minimal shrinkage. Epoxy resins are typically cured using a cationic initiator, such as an aryl sulfonium or iodonium salt, which follows a step-growth polymerization mechanism, as supported by previous studies [14]. The oligomer selected for this research was Ebecryl 3700 BPA epoxy resin, chosen for its excellent hardness and temperature resistance. Additionally, Trimethylolpropane Triacrylate (TMPTA) was introduced to the formulation to reduce the viscosity, making it easier to handle during the printing process.

To initiate the polymerization process, which cannot occur with light exposure alone, two distinct photo-initiators were incorporated into the resin formulations. These were Phenylbis 2,4,6 Trimethyl Benzoyl Phosphine Oxide (BAPO) and Diphenyl (2,4,6-trimethyl benzoyl) phosphine oxide (TPO-L). Three distinct formulations were prepared for the study: one with neat Ebecryl resin and two others containing nano-silica at 5 wt% and 10 wt% concentrations, respectively, to form nanocomposites. Table 1 outlines the detailed composition of the neat and nanocomposite formulations. The goal was to evaluate how the inclusion of nano-silica affects the mechanical properties of the printed parts in comparison to the neat epoxy formulation.

Table 1: Specifications for Nanocryl A220

Property	Units	Typical Values
Base Acrylate	-	Trimethylolpropane triacrylate (TMPTA)
SiO2 Content	wt%	~ 50
Density	g/ml	~ 1.3
Viscosity	mPas	~ 2000

2.2 Resin Preparation

The resin mixture preparation began by heating the Ebecryl 3700 BPA Epoxy resin (sample from Allnex GMBH) to approximately 70°C to reduce its viscosity, making it easier to handle. Once the desired consistency was achieved, the resin was combined with the oligomer Trimethylolpropane Triacrylate (TMPTA) (sample from ALlnex GMBH) in a container. Pre-calculated amounts of Nanocryl A 220 (sample from Evonik Operations GmbH) were introduced to achieve 5 wt% and 10 wt% silica loadings for the formulations containing nano-silica. Nanocryl A220 is a high-performance dispersion comprising colloidal silica in a trifunctional acrylate monomer, designed for adhesive applications. Despite its high SiO2 content of around 50 wt%, Nanocryl A220 maintains excellent transparency and low viscosity, with no sedimentation, thanks to the well-dispersed nanoparticles in the acrylate matrix. The next step involved adding the photo-initiators, Phenylbis 2,4,6 Trimethyl Benzoyl Phosphine Oxide (BAPO) and Diphenyl (2,4,6-trimethyl benzoyl) phosphine oxide (TPO-L), to initiate the curing reaction during exposure to light.

Once all components were added, the resin mixture was first hand-stirred using a stirring stick to ensure initial blending. Following this, a Thinky Planetary Vacuum Mixer was employed to mix the resin at 2000 rpm for 10 minutes under a vacuum pressure of -99 KPa. This step was critical for thoroughly dispersing the nano silica and removing any air bubbles from the resin mixture, ensuring homogeneity and eliminating potential defects in the final 3D-printed parts.

Table 2: Neat and Nano Silica-infused nanocomposite resin formulations

Formulations	EBECRYL 3700 BPA (g)	TMPTA (g)	BAPO (g)	TPO-L (g)	Nanocryl A220 (g)
Neat Resin	20 (40 wt%)	29 (58 wt%)	1 (2 wt%)	-	-
5 wt% SiO_2	20	27	0.25	0.25	5
10 wt% SiO_2	20	24.5	0.25	0.25	10

2.3 Specimen Printing

The printing of tensile, flexural, and coefficient of thermal expansion (CTE) specimens was performed using an Anycubic Photon D2 DLP printer, which operates at a wavelength of 405 nm with a pixel resolution of 62 µm in the x−y plane. The printing process involved a layer thickness of 0.05 mm, with the specimens oriented flatwise in the x−y direction, ensuring that the length of the specimens was aligned along this plane. This configuration allows for high precision and reproducibility in the printed specimens.

To optimize the curing times for the different specimens, preliminary experiments were conducted using a coin design featuring intricate details with feature sizes up to 500 micrometers. The clarity of these features was used to determine the appropriate curing times. The final curing times for the Neat, 5 wt%, and 10 wt% nano silica loading levels were established based on these experimental results. These curing times are detailed in Table 3, reflecting the adjustments made to ensure optimal print quality and material performance for each formulation.

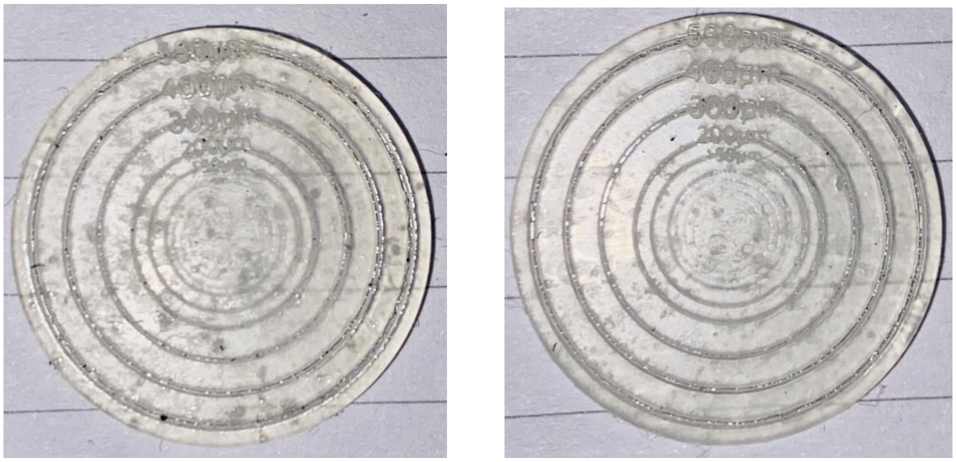

Figure 2: Coin structures for 5wt% and 10 wt% loading levels of SiO_2

Table 3: Prinitng parameters for Ebecryl Near, 5 wt% and 10 wt% loading of Nano Silica

Formulation	Printing Setting	Layer Height (mm)	Curing Time (s)	Pause Time Before Print (s)	Bed Lift Speed (µm / Second)
Neat Resin	Burn-in Layers	0.05	10	0.1	200
	Normal Layers	0.05	8	0.1	200
5 wt% SiO_2	Burn-in Layers	0.05	25	0.1	200
	Normal Layers	0.05	12	0.1	200
10 wt% SiO_2	Burn-in Layers	0.05	25	0.5	200
	Normal Layers	0.05	13	0.5	200

2.4 Characterization.

2.4.1 Mechanical Properties

The tensile properties of both the neat resin and the nanocomposite resin were evaluated using an MTS Exceed Series 40 Electromechanical Testing System, manufactured by MTS Systems. The tensile specimens were printed according to the ASTM D638 "Standard Test Method for Tensile Properties of Plastics," specifically using Type IV geometry. The overall sample dimensions were 115 mm in length, with a narrow section width of 6 mm and a thickness of 3.2 mm. Tensile testing was conducted at a strain rate of 0.2 inches per minute, and the gauge length of the specimens was accurately measured using a digital slide caliper to ensure precise data collection.

The flexural properties of the neat resin and nanocomposite resin were tested using a UTS Electromechanical Test System, manufactured by UnitedTest in Beijing, China. The specimens were printed following ASTM D790 "Standard Test Method for Flexural Properties of Unreinforced and Reinforced Plastics and Electrical Insulating Materials." Each sample measured 125 mm in length, 12.7 mm in width, and 3.2 mm in thickness. Flexural testing was carried out at a strain rate of 0.2 inches per minute, with the gauge length of the specimens precisely measured using a digital slide caliper to ensure accuracy in the data collection process.

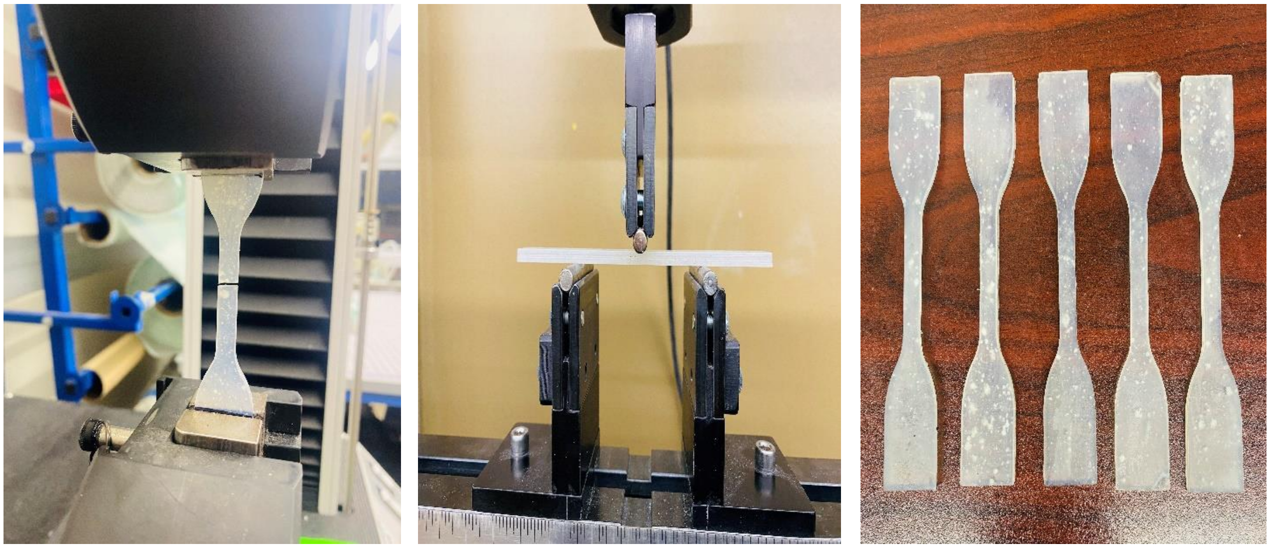

Figure 3: Tensile testing via United Testing System (UTS) setup (left), 3-point bend test via Material Testing System (MTS)(middle), and SLA 3D printed samples(right)

2.4.4 Thermal Properties

The thermo-mechanical properties of the neat Ebecryl resin and the nano silica (SiO_2) infused resin were analyzed using Dynamic Mechanical Analysis (DMA) with the TMA Q400 System from TA Instruments (New Castle, Delaware, USA) in macro expansion mode. The testing was conducted over a temperature range from 30 °C to 150 °C, with a heating rate of 5 °C per minute, and a frequency of 0.5 Hz. The thermo-mechanical analysis was performed following the guidelines of ASTM E831-19, "Standard Test Method for Linear Thermal Expansion of Solid Materials by Thermomechanical Analysis," ensuring accurate measurement of thermal expansion behavior across the specified temperature range.

The mean coefficient of thermal expansion (CTE) was calculated using the following equation as per ASTM E831-19:

$$\alpha_m = \frac{\Delta Lsp \times k}{L \times \Delta T}$$

where:

- α_m = mean coefficient of linear thermal expansion, µm/(m·°C),

- k = calibration coefficient, from Test Method E2113,
- L = specimen length at room temperature, m,
- ΔLsp = change of specimen length, µm,
- ΔT = temperature difference over which the change in specimen length is measured, °C,
- T = midpoint temperature of the temperature range ΔT

Figure 4: Mounted CTE sample on the TA Instruments TMA Q400

3. RESULTS AND DISCUSSION

3.1 Mechanical Properties

Table 4 presents the mechanical properties data as obtained from testing of the specimens. Five different specimens were tested to generate each value which is their average. The results demonstrate the performance of the SLA 3D printed specimens under tensile and flexural mechanical loading.

From the comparison of tensile properties for the three resin systems—Ebecryl Neat, 5 wt% SiO_2, and 10 wt% SiO_2—reveals significant differences in their mechanical performance due to the incorporation of silica nanoparticles. The ultimate tensile strength decreases with the addition of silica, dropping from 16.45 MPa for Ebecryl Neat to 14.15 MPa for 5 wt% SiO_2 and further to 13.35 MPa for 10 wt% SiO_2. This trend suggests that increasing silica content creates stress concentration points within the resin matrix, which can act as initiation sites for cracks, thereby slightly compromising the tensile strength. In contrast, the tensile modulus shows an increase with silica addition, rising from 342.09 MPa for Ebecryl Neat to 597 MPa for 5 wt% SiO_2 and 625 MPa for 10 wt% SiO_2. This behavior is attributed to the high stiffness of silica nanoparticles, which restricts the mobility of polymer chains, leading to an overall increase in the rigidity of the composite. However, the percentage of elongation decreases markedly with increased silica content, from 5.61% for the neat resin to 2.46% for the 5 wt% SiO_2 and further to 2.19% for the 10 wt% SiO_2. This reduction in elongation reflects a decline in ductility, suggesting that the presence of rigid silica particles reduces the polymer matrix's ability to deform under tensile stress, thereby making the material more brittle.

Table 4: Mechanical properties of Ebecryl neat/SiO_2-infused SLA 3D resin

Mechanical Properties	Ebecryl Neat	5 wt% SiO_2	10 wt% SiO_2
Ultimate Tensile Strength (MPa)	16.45	14.15	13.35
Tensile Modulus (MPa)	342.09	597	625
Percentage of Elongation (%)	5.61	2.46	2.19
Flexural Strength (MPa)	18.65	33.61	18.77
Flexural Modulus (MPa)	459.01	978.24	586.94

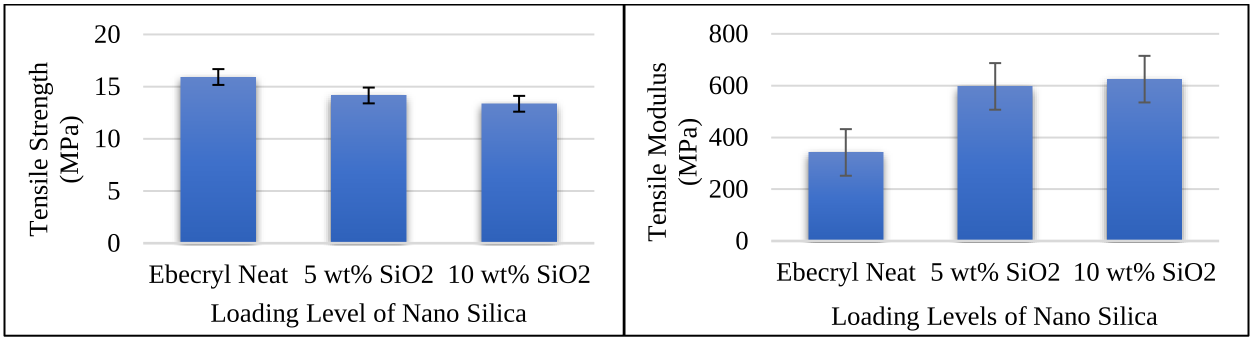

Figure 5: Tensile strength and modulus of different loading levels of Nano Silica compared to neat resin

As for the flexural properties of Ebecryl Neat, 5 wt% SiO_2, and 10 wt% SiO_2 they exhibit notable variations that align with the changes observed in their tensile properties. The flexural strength increases significantly with the addition of silica, from 18.65 MPa for Ebecryl Neat to 33.61 MPa for 5 wt% SiO_2, suggesting that silica reinforcement enhances the material's resistance to bending stresses. However, at 10 wt% SiO_2, the flexural strength slightly decreases to 18.77 MPa, which may be due to agglomeration of silica particles at higher loading levels, resulting in stress concentration points and reduced strength, similar to the trend observed in tensile strength. The flexural modulus follows a trend similar to the tensile modulus, increasing from 459.01 MPa for Ebecryl Neat to 978.24 MPa for 5 wt% SiO_2 and then slightly decreasing to 586.94 MPa at 10 wt% SiO_2. The initial increase in modulus with silica addition can be attributed to the stiffening effect of the rigid silica particles, which restricts polymer chain mobility and enhances rigidity under bending loads. However, the decrease at higher loading levels could be related to particle aggregation, which impairs the uniform stress distribution across the matrix. The reduction in flexural strength and modulus at higher silica contents mirrors the decrease in tensile strength and elongation, indicating that excessive silica may lead to brittleness and stress localization, ultimately affecting both tensile and flexural performance.

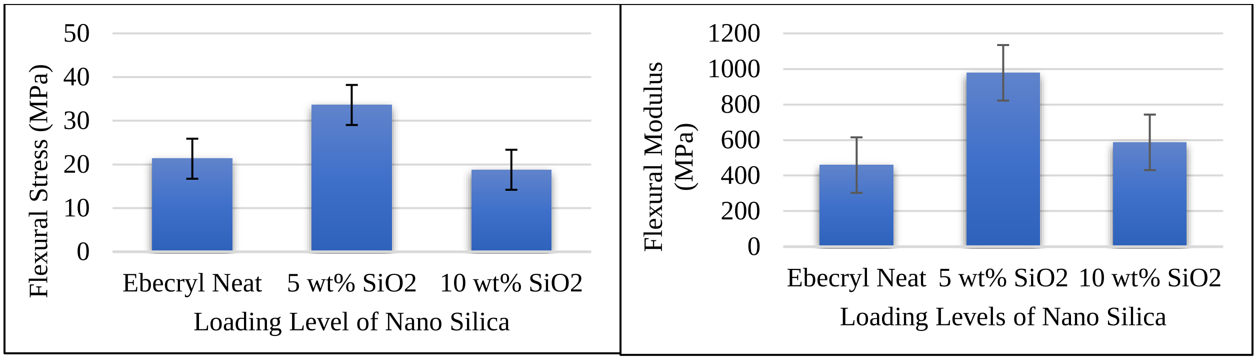

Figure 6: Flexural strength and modulus of different loading levels of Nano Silica compared to neat resin

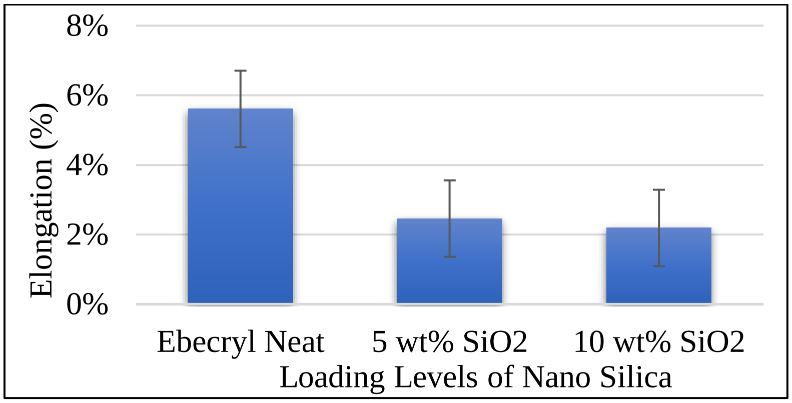

Figure 7: % Elongation for different loading levels of Nano Silica compared to neat resin

From the stress vs strain curves for Ebecryl Neat, 5 wt% SiO_2, and 10 wt% SiO_2 resin systems. Ebecryl Neat shows a more ductile behavior with a higher strain at break, reaching over 0.05 strain, indicating its ability to stretch significantly under tensile loading. However, its stress capacity is lower, with a maximum tensile stress of around 16 MPa. In contrast, both the 5 wt% and 10 wt% SiO_2 samples exhibit steeper initial slopes, indicative of higher tensile moduli, which correspond to increased stiffness. The incorporation of silica nanoparticles enhances the rigidity of the resin matrix, resulting in reduced elongation, with the 10 wt% SiO_2 showing the least strain at break. However, these reinforced systems also exhibit a decrease in maximum tensile stress compared to the neat resin, likely due to stress concentration points created by the silica particles, leading to earlier fracture. This behavior suggests a trade-off between stiffness and tensile strength when adding silica to the resin matrix.

As from the load vs. deflection curves for the three resin systems, Ebecryl Neat shows the highest deflection, indicating its relatively lower stiffness and higher flexibility under bending loads. On the other hand, the 5 wt% SiO_2 resin demonstrates a significantly higher load-bearing capacity and reduced deflection, highlighting the improved flexural strength and stiffness imparted by the silica reinforcement. The 10 wt% SiO_2 sample follows a similar trend but with a slightly lower maximum load capacity than the 5 wt% sample, possibly due to the agglomeration of silica particles at higher concentrations, which can act as stress concentrators and reduce the overall strength. The changes in the flexural behavior align with the tensile test results, where the addition of silica enhances the stiffness but reduces the material's ability to deform, leading to a more brittle nature.

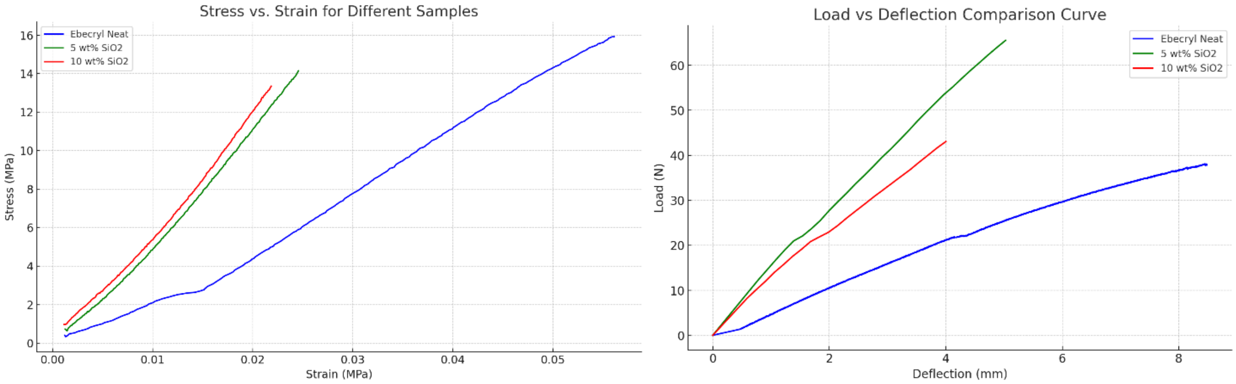

Figure 8: Stress-strain curve (L) and load-deflection curve (R) for different specimens

3.3 Thermo Mechanical Analysis

The table compares the coefficient of thermal expansion (CTE) of Ebecryl Neat resin with resins containing 5 wt% and 10 wt% silica (SiO_2) at 150 °C, alongside Nickel as a reference. The Ebecryl Neat resin exhibits the highest CTE at 109.48 µm/m°C, serving as the baseline measurement. The addition of SiO_2 significantly reduces the CTE, indicating improved thermal stability. Specifically, the 5 wt% SiO_2 resin shows a 25% reduction in CTE, decreasing to 81.88 µm/m°C, while the 10 wt% SiO_2 resin results in a 36% reduction, bringing the CTE down to 69.52 µm/m°C. This reduction in CTE with increased silica content can be attributed to the inherent low thermal expansion of silica particles, which act as a reinforcing filler, restricting the expansion of the resin matrix. Additionally, the strong interfacial bonding between the silica particles and the polymer matrix contributes to the reduced thermal expansion. In comparison, Nickel has a much lower CTE of 13.3 µm/m°C, reflecting an 87.85% reduction relative to the neat resin, which underscores the effectiveness of incorporating materials with low thermal expansion to enhance the thermal dimensional stability of composite systems.

Table 5: Comparison of mean CTE values of different resin systems with Nickel

Material	CTE (µm/m°C) at 150 °C	Percent Change
Ebecryl Neat	109.48	Baseline Measurement
5 wt% SiO_2	81.88	25% reduction
10 wt% SO_2	69.52	36% reduction
Nickel	13.3	87.85% reduction

The deflection versus temperature curve shows that Ebecryl Neat has the highest deflection across the temperature range, indicating its high coefficient of thermal expansion (CTE). In contrast, the resins with 5 wt% and 10 wt% SiO_2 exhibit significantly lower deflections, with the 10 wt% SiO_2 resin displaying the least deflection. This trend aligns with the earlier CTE data, confirming that the incorporation of silica particles restricts the polymer matrix's thermal expansion. The reduction in deflection with increasing SiO_2 content can be attributed to the stiff, thermally stable nature of the silica particles, which reduces the overall thermal movement of the composite.

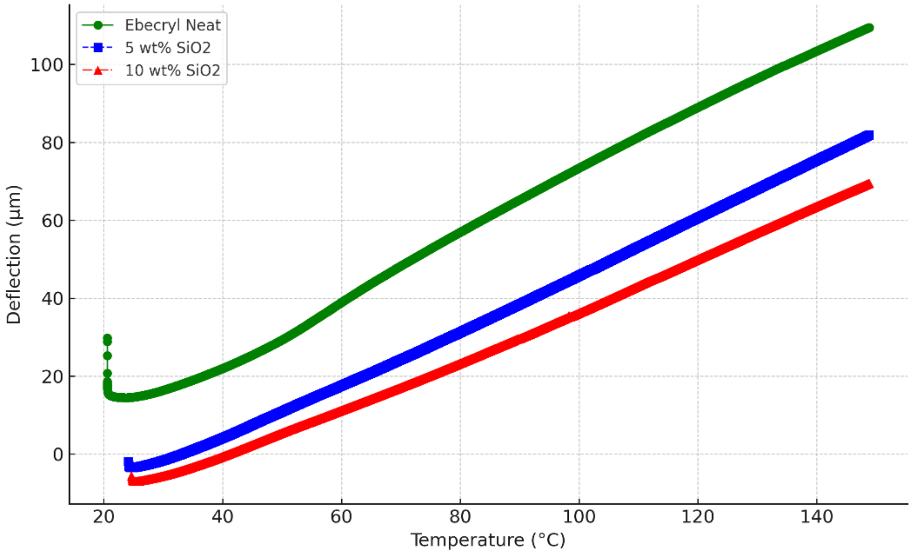

Figure 9: Comparison of Coefficient of Thermal Expansion for different loading levels of SiO_2

4. CONCLUSIONS

In conclusion, the tensile properties of the resin systems show that the addition of silica particles affects both strength and ductility. The neat Ebecryl resin exhibits the highest elongation, indicating its malleable nature, but it has lower tensile strength compared to the reinforced systems. Incorporating 5 wt% and 10 wt% SiO_2 improves the stiffness of the resin, as evidenced by the increased tensile modulus. However, this comes at the cost of reduced tensile strength and ductility, with higher silica content leading to more pronounced brittleness. Despite this, the reinforcement provides enhanced rigidity, which is beneficial for applications requiring materials with higher structural integrity.

The flexural properties follow a similar trend. The neat Ebecryl resin shows more flexibility under bending loads, while the 5 wt% SiO_2 resin demonstrates the highest flexural strength, indicating that a moderate amount of silica reinforcement significantly enhances the material's resistance to bending. However, at 10 wt% SiO_2, the flexural strength slightly decreases, likely due to particle agglomeration leading to stress concentration points. Additionally, both reinforced systems show increased flexural modulus, confirming the role of silica in restricting the polymer matrix's deformation. This stiffening effect is crucial for applications where rigidity and mechanical durability are essential.

In terms of thermal properties, the addition of SiO_2 significantly lowers the coefficient of thermal expansion (CTE), with the 10 wt% SiO_2 resin achieving the greatest reduction. The reduction in CTE indicates improved thermal stability, making the reinforced resins more suitable for environments with varying temperatures. Given the analysis of both mechanical and thermal properties, the 5 wt% SiO_2 resin emerges as the most balanced option. It offers a substantial reduction in CTE while maintaining better mechanical properties than the 10 wt% SiO_2 resin, which becomes more brittle. Therefore, the 5 wt% SiO_2 resin is best suited for applications requiring a low CTE without compromising much on mechanical performance.

5. ACKNOWLEDGEMENT

The authors are thankful to all the members of the Advanced Composites Lab (ACL) at Texas State University for their help with its state-of-the-art facility. Special thanks are also given to the Shared Research Operations Center (SRO) of Texas State University for the access to its facilities. The authors would like to thank Mr. Abhay Deshpandey of Evonik Corporation for providing a free sample of Nanocryl A220 for this research. The authors would like to acknowledge support from Texas State University through a Thesis Research Support Fellowship for this research.

6. REFERENCES

[1] Jacobs, P. F. (1992). Rapid Prototyping & Manufacturing: Fundamentals of Stereolithography, Society of Manufacturing Engineers - One SME Drive, Dearborn, MI.

[2] Chockalingam, K., Jawahar, N. and Chandrasekhar, U. (2006). Influence of Layer Thickness on Mechanical Properties in Stereolithography, Rapid Prototyping J., 12: 106–113

[3] Gan, Z. W., Mo, J. H., Huang, S. H. and Xie, H. Q. (2006). Development of a Hybrid Photopolymer for Stereolithography, J. Wuhan Univ. Technol., 21: 99–101.

[4] Huang, Y. M., Kuriyama, S. and Jiang, C. P. (2004). Fundamental Study and Theoretical Analysis in a Constrained-surface Stereolithography System, Int. J. Adv. Manuf. Technol., 24: 361–369.

[5] Zhou, J. G., Herscovici, D. and Chen, C. C. (2000). Parametric Process Optimization to Improve the Accuracy of Rapid Prototyped Stereolithography Parts, Int. J. Mach. Tool. Manuf., 40: 363–379.

[6] Zixiang Weng, Yu Zhou, Wenxiong Lin, T. Senthil, Lixin Wu, Structure-property relationship of nano-enhanced stereolithography resin for desktop SLA 3D printer, Composites Part A: Applied Science and Manufacturing, Volume 88, 2016, Pages 234-242, ISSN 1359-835X,

[7] Gonon, P., Sylvestre, A., Teysseyre, J. *et al.* Dielectric properties of epoxy/silica composites used for microlectronic packaging, and their dependence on post-curing. *Journal of Materials Science: Materials in Electronics* **12**, 81–86 (2001)

[8] Schapery RA. Thermal Expansion Coefficients of Composite Materials Based on Energy Principles. *Journal of Composite Materials*. 1968;2(3):380-404

[9] Chow, T.S. (1978), Effect of particle shape at finite concentration on thermal expansion of filled polymers. J. Polym. Sci. Polym. Phys. Ed., 16: 967-970

[10] Dittanet, Peerapan & Pearson, Raymond. (2012). Effect of silica nanoparticle size on toughening mechanisms of filled epoxy. Polymer. 53. 1890–1905. 10.1016/j.polymer.2012.02.052.

[11] . González-Benito, E. Castillo, J.F. Caldito, Coefficient of thermal expansion of TiO2 filled EVA based nanocomposites. A new insight about the influence of filler particle size in composites, European Polymer Journal, Volume 49, Issue 7, 2013, Pages 1747-1752,

[12] Shariff, Assoc. Prof. Dr. Khairul & Jaafar, Mariatti & Azizan, A. & Mang, N. & Tham, W.. (2011). Effect of different types of silver and epoxy systems on the properties of silver/epoxy conductive adhesives. Journal of Materials Science: Materials in Electronics. 22. 757-764. 10.1007/s10854-010-0207-7.

[13] Lisa M. Sullivan and Charles M. Lukehart. Zirconium Tungstate (ZrW_2O_8)/Polyimide Nanocomposites Exhibiting Reduced Coefficient of Thermal Expansion *Chemistry of Materials* **2005** *17* (8), 2136-2141

[14] Samuel Clark Ligon-Auer, Martin Schwentenwein, Christian Gorsche and Rober Liska. Toughening of photo-curable polymer networks: a review, Journal of Polymer Chemistry Issue 2, 2016, 7, 257-286